Mikrochim. Acta 131, 75–83 (1999)

Mikrochimica Acta

Printed in Austria

Whole Blood Diagnostics in Standard Gravity and Microgravity by Use of Microfluidic Structures (T-Sensors)

Bernhard H. Weigl[2,*], **Jennah Kriebel**[1], **Kelly J. Mayes**[1], **Todd Bui**[1], and **Paul Yager**[1]

[1] Department of Bioengineering, University of Washington, Box 352141, Seattle, WA 98195, USA
[2] Micronics, Inc., Redmond, WA 98052, USA

Abstract. In channels with dimensions much less than 1 mm, fluids with viscosities similar to or higher than that of water and flowing at low velocities exhibit laminar behavior. This allows the adjacent flow of fluids and particles in a channel without mixing other than by diffusion. We demonstrate here the use of a 3-input microfluidic device known as a T-Sensor for the analysis of blood. A sample solution (e.g. whole blood), a receptor solution (e.g. an indicator solution), and a reference solution (a known analyte standard) are introduced into a common channel (T-Sensor), and flow side by side until they leave the structure. Smaller particles such as ions or small proteins diffuse rapidly across the fluid boundaries, whereas larger molecules diffuse more slowly. Large particles (e.g. blood cells) show no significant diffusion within the time the flow streams are in contact. Two interface zones are formed between the fluid layers. The ratio of a property (e.g. fluorescence intensity) of the outer portions of the two interface zones is a function of the concentration of the analyte, and is largely free of cross-sensitivities to other sample components and instrument parameters. This device allows, for example, one-time or continuous monitoring of the concentration of analytes in microliters of whole blood without the use of membranes or prior removal of blood cells. The principle is illustrated by the determination of pH and human albumin in whole blood and serum. Results are also presented for zero-gravity experiments performed with a T-Sensor on board a NASA experimental plane. Due to its microfluidic flow characteristics, a T-Sensor functions independently of orientation and strength of the gravitational field. This was demonstrated by exposing a T-Sensor to variations in gravity from 0 to 1.8 g in a NASA KC135A plane flying repetitive parabolic flight curves.

Key words: blood diagnostics; microfluidics; microgravity; T-Sensors.

Over the past five years, several research groups have begun to manufacture flow structures and fluid handling devices with feature sizes in the low μm range [1–4]. Such devices can be mass produced in silicon by techniques such as anisotropic etching or reactive ion etching, or made out of plastics by use of casting, cutting, and stamping techniques. It is expected that analytical devices based on microfabricated devices will soon be in widespread use [3, 4]. Such devices offer many advantages over traditional analytical devices, such as low sample consumption, cheap unit prices and disposability, but also have distinctive properties inherent to their small dimensions. Facts relevant to the sensor presented in this paper are: (a) aqueous flow in microchannels can easily be made laminar; (b) in small channels diffusion is an efficient process for mixing fluids; (c) particles can be separated by diffusion according to their size.

Diffusion-Based Mixing and Separation

Molecules, ions, and small particles diffuse rapidly over typical microfabrication dimensions. The dis-

* To whom correspondence should be addressed

tance l that a typical spherical particle will diffuse in time t is described by $l = (Dt)^{0.5}$. D is the diffusion coefficient, given by

$$D = \frac{RT}{N}\frac{1}{3\pi\eta d} \quad (1)$$

where $R = 8.31 \times 10^7, N = 6.02 \times 10^{23}$, T is the absolute temperature, η is the solvent viscosity, and d is the particle diameter. For example, at room temperature in aqueous solution, a spherical molecule with a molecular weight of 330 takes 0.2 s to diffuse 10 µm, whereas a bead with a diameter of 0.5 µm takes about 200 s to cover the same distance [5–7]. This effect can be used to separate molecules and particles according to their size [8], and is particularly useful in microfabricated devices [9–11].

Laminar Flow

The Reynolds number is a non-dimensional parameter relating the ratio of the inertial to viscous forces in a specific fluid flow configuration, and is defined as:

$$\mathrm{Re} = \frac{\rho\nu w}{\mu} \quad (2)$$

where ρ is the fluid density, ν is the mean flow velocity, μ is the fluid viscosity, and w is the characteristic dimension of the flow geometry. In microfabricated devices, w is small compared to most macroscopic flow geometries. If the Reynolds number of two fluid streams are the same the flows are said to be hydrodynamically similar. An aqueous flow stream in a microchannel is hydrodynamically similar to a very viscous oil-like stream in a significantly larger channel because the viscosity of the oil is much larger than that of water [2]. The Reynolds number for aqueous fluids in µm-sized channels can be much less than unity at low flow rates. Low Reynolds number flow is always laminar; therefore, even though two fluids may be miscible turbulent mixing does not occur. In the absence of turbulence or stable recirculation zones it is possible for two streams of similar viscosity to flow adjacent to one another in a linear path down a flow channel with minimal dispersive mixing [2, 6–8], as shown in Fig. 1.

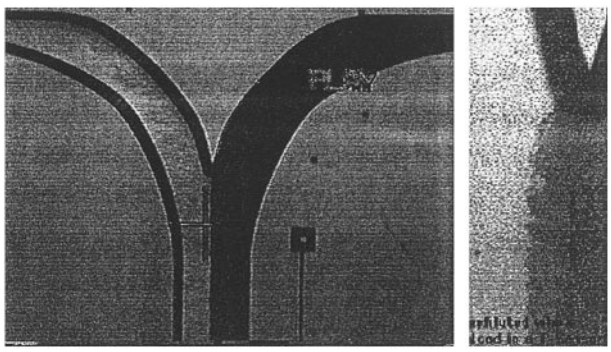

Fig. 1. Example of two laminar flow streams, one being whole blood, the other phosphate buffered saline) next to each other in a T-shaped channel; the image to the right was taken at the T-joint with a higher magnification at near-stop-flow conditions

Self-Referencing Diffusion-Based Detection

Many detection methods require that the sample analyte be separated from insoluble sample components, and from other components to which the detection system is sensitive. In the flow structures

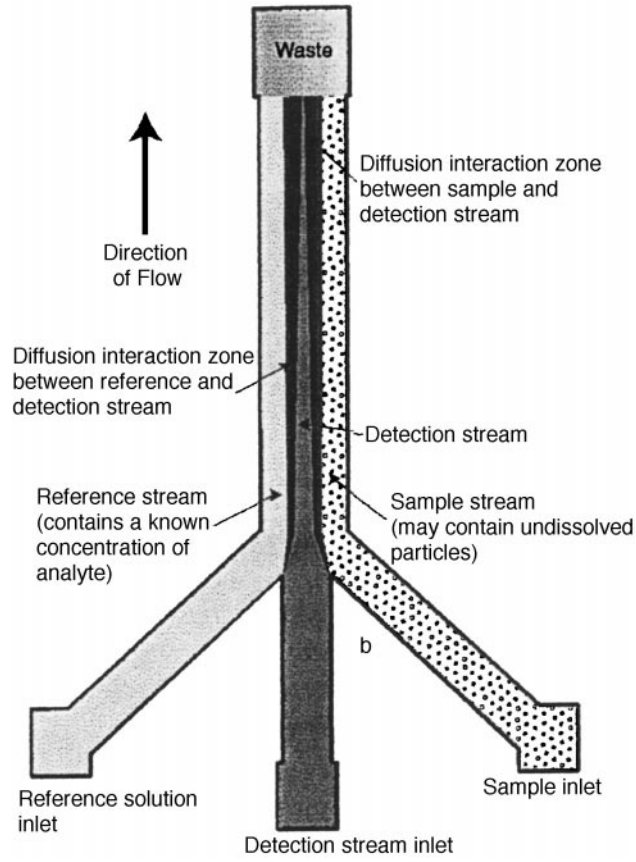

Fig. 2. Schematic of flow and diffusion within the T-Sensor at a 1:1:1 flow ratio. A reference stream enters the device from the left bottom inlet port, a detection (indicator stream) from the central port and a sample stream enters from the bottom right port. All streams flow in parallel after the T-junction of the central detection channel. The detection channel stream exists at the port shown at the top

presented here, we rely on both *laminar flow* and *diffusion-based mixing and separation* to detect a single analyte in a complex sample [12–15]. Into a Ψ-shaped micro-channel channel system, consisting of three ''tributary'' channels and a detection channel, a sample solution, a detection solution, and a reference solution are introduced at the channel junction. The three streams flow next to each other until they leave the structure.

Ions such as H^+ and Na^+ and small molecules diffuse rapidly across the fluid boundaries between adjacent streams, whereas larger molecules diffuse more slowly. All three solutions are aqueous, so the diffusional exchange of water has no net effect. Very large molecules and insoluble particles such as blood cells show no significant diffusion within the time the three flow layers are in contact in the common channel. In the schematic in Fig. 2, the right-hand stream is an unknown sample solution containing a mixture of soluble and insoluble particles (e.g. human blood). The middle stream is a solution containing the detection reagent (e.g. a fluorescent indicator). The left-hand stream is a reference solution containing a known concentration of the analyte. Due to the diffusion of analyte particles from both the sample and the reference into the detection solution, as well as the diffusion of indicator molecules into both adjacent streams, and the subsequent reaction of analyte particles with the detection solution, diffusion interaction zones form between the fluid layers. If an indicator is used in the detection solution, the diffusion interaction zones will be optically detectable, the optical signal being a function of the concentration of the analyte. Figure 3 shows a micrograph in which control, indicator, and sample

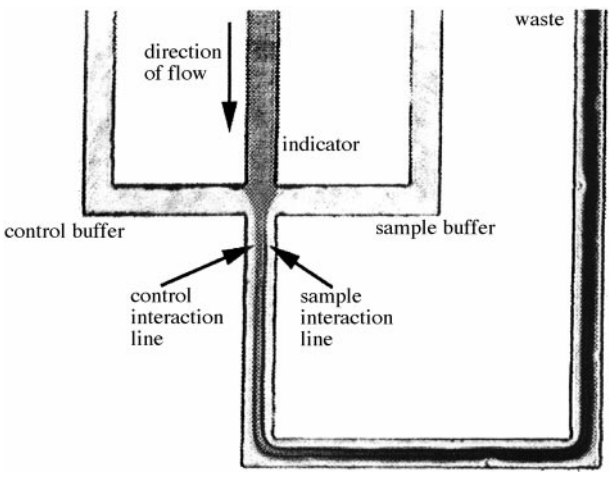

Fig. 3. Control (buffer pH 7), indicator (Bromocresol Purple), and ''sample'' (buffer pH 9) solutions flow in parallel in a T-Sensor channel, and display the behavior outlined in Fig. 2. The channel diffusion dimension d is 500 µm, and width (optical path-length) is 100 µm. The image was taken with a CCD camera with a macro objective

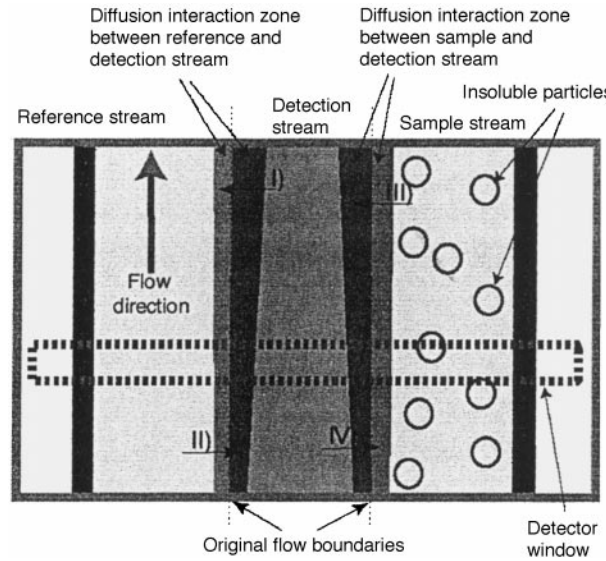

Fig. 4. Schematic showing a magnified section of the detection channel, including the detector window

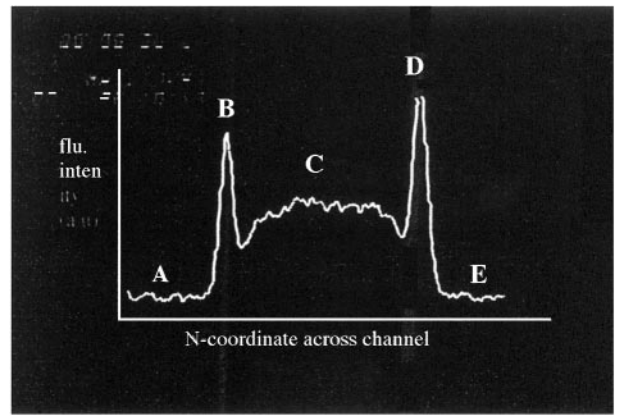

Fig. 5. Fluorescence micrograph of a detection channel section containing a control, indicator, and sample streams during a determination of human serum albumin, superimposed on which is a corresponding light intensity profile. Please note that in the case of the fairly large albumin molecule and the much smaller indicator dye molecule, the formation of the interaction zone is largely due to diffusion of indicator into the sample. The following values can be used for data reduction and referencing:
A: reference background;
B: reference interaction zone intensity;
C: detection solution background;
D: sample interaction zone intensity;
E: sample background

solutions flow next to each other in a T-Sensor structure, and display the behavior outlined in Fig. 2.

Figure 4 shows a magnified section of the schematic in Fig. 2. It shows the formation of the diffusion interaction zones. Figure 5 is a micrograph of a detection channel containing a control, indicator, and sample during a determination of human serum albumin. Superimposed on the image is the corresponding light intensity histogram, which can be used to quantify concentrations in both the control and sample stream. As a model diagnostic test for this paper, we tested the use of an optical absorption-based T-Sensor determination of pH in whole blood.

Experimental

Silicon Manufacturing

Silicon microchannels were used for the fluorescence experiment shown in the introduction to this paper (Fig. 4). Silicon micromachining was performed in the facilities of the Washington Technology Center at the University of Washington as described by Brody and Yager [2].

Polymer Microfabrication

All optical absorption experiments were performed in Mylar laminate-based plastic microstructures manufactured by Micronics, Inc. An array of structures was laser-cut out of 8.5 in. × 11 in. sheets of Mylar (3M, Austin, TX) and separated into individual microfluidic units with a laser cutter (ULS-25E Universal Laser Systems, Scottsdale, AZ). The cut pieces were then laminated on both sides with Mylar cover slides, and inserted into a flow cell adapter. The structural dimensions were: channel depth 100 μm, width 500 μm, length of measurement channel 20 mm.

Fluid Flow Rate Control

A customized control station consisting of three computer controlled syringe pumps (Kloehn Company, Ltd., Las Vegas, NV) was used to provide constant flow rates in the microstructures used in the laboratory experiments.

Optical Detection

A Zeiss ICM 405 inverted microscope (Carl Zeiss Co., Jena, Germany) was equipped with fluorescence filter sets (for fluorescence experiments only), and a color video camera. The silicon device was attached to the stage of the microscope. Video images were taken for each sample in each channel. The images were then digitized, transferred to a PowerMac 8100 AV (Apple Computer Co, Cupertino, CA), and processed with NIH image and Adobe PhotoShop software (Adobe Systems, Inc., San Jose, CA), using custom image-processing macros.

Data Reduction

After acquisition of the original digital image, a portion of the image was selected for data processing (see Fig. 4). First, the intensity of several lines of pixels (typically 5) across the channel was averaged. Then, the cross-section was divided into several zones (see Fig. 5): reference background (A), reference interaction zone intensity (B), detection solution background (C), sample interaction zone intensity (D), and sample background (E).

The reference, sample, and detection solution backgrounds were determined by averaging predefined sections of the flat portions of the light intensity cross-section graph. The reference interaction zone and sample interaction zone maximum intensities were determined with Gaussian-fit routines. While many different combinations of these derived values can be used in analyzing the data, for the experiments described below the sample

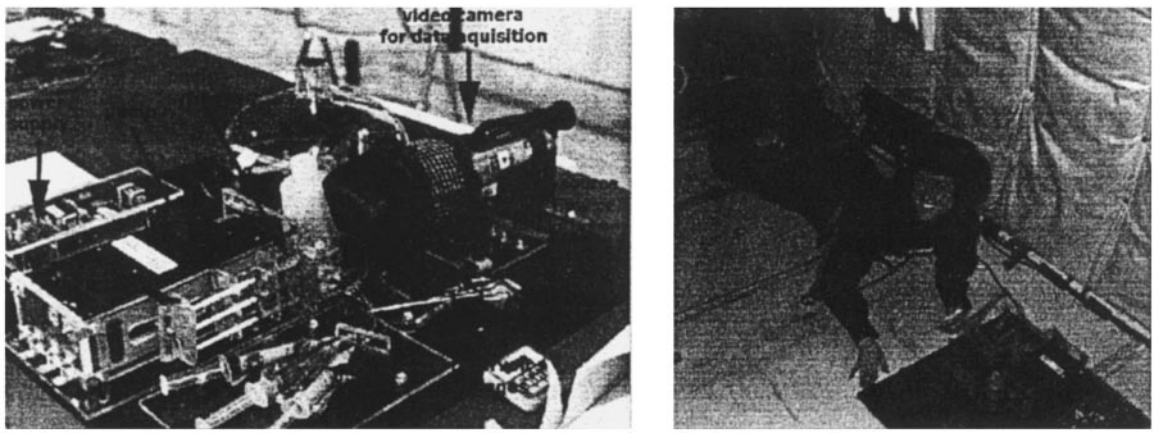

Fig. 6. (Left) Experimental set-up consisting of pumps, light source. T-Sensor cell, and CCD camera as a detector; (right) Jennah operating the experiment in a microgravity phase

concentration was derived from the ratio of the sample interaction zone intensity (D) to the reference interaction zone intensity (B).

Sample Preparation

All chemicals and buffers used were obtained from Aldrich Chemical Co., Milwaukee, WI, unless otherwise noted. Whole heparinized blood and serum were obtained from University of Washington Medical Center patients with authorization by an internal review committee according to the ethical standards of the Helsinki Declaration of 1975 and its 1983 revision. The indicator for the absorption-based pH experiments was Bromocresol Purple [Bromocresol Purple solution (saturated at 25 °C) diluted tenfold with 140 mM NaCl in demineralized water]. For fluorescence-based experiments, the indicator dye Albumin Blue 580 was used (Molecular Probes Inc., Eugene, OR). The indicator solution was made by first saturating isopropyl alcohol with Albumin Blue 580 at 25 °C, and then diluting the mixture 1:50 with 140 mM NaCl solution in demineralized water.

Microgravity Experiments

A custom-made portable T-Sensor station (Fig. 6, left) consisting of a modified 3-syringe pump (Kloehn Company, Ltd., Las Vegas, NV), a laminate T-Sensor flow cell, an electroluminescent light source (Proto-Kut, from Edmond Scientific, Inc., Barrington, NJ), and a consumer-grade Sony Hi-8 video camera, was mounted on the floor of a NASA KC135 A experimental aircraft (Fig. 7 left). The plane performed 2 series of 50 parabolic flight curves on two consecutive days. Each flight curve consisted of 40 s of 1.8 g, followed by 25 s of near microgravity (Fig. 7 right). The experiment was operated manually during the flights.

Results and Discussion

Figure 8 shows the results of an experiment to determine the effects of varying viscosity on the flow pattern in a T-Sensor. In each image, the control solution [phosphate-buffered saline (PBS) at pH 7.4] enters the structure from the left, the indicator (a Bromocresol Purple solution) enters from the top, and the sample (left image buffer; middle image blood diluted with 10 parts PBS; right image whole blood) from the right. The viscosity of the sample solutions increases from buffer to diluted blood to whole blood; the diluted blood is about 1.5 times more viscous, and whole blood about 4.5 times more viscous than the buffer. Positive displacement pumps were used to

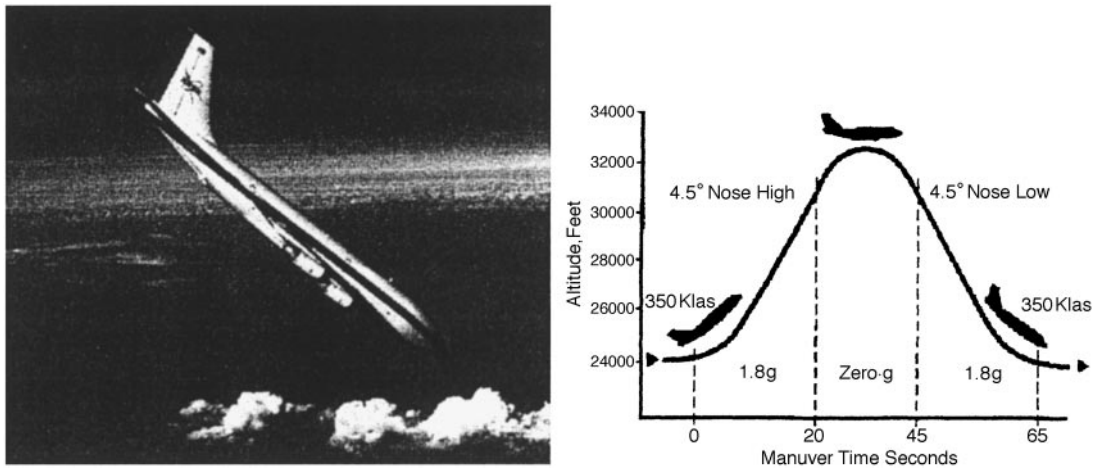

Fig. 7. The KCl35A, the military equivalent of a Boeing 707, during a microgravity free-fall phase (left), and its flight curve during the T-Sensor experiment (right)

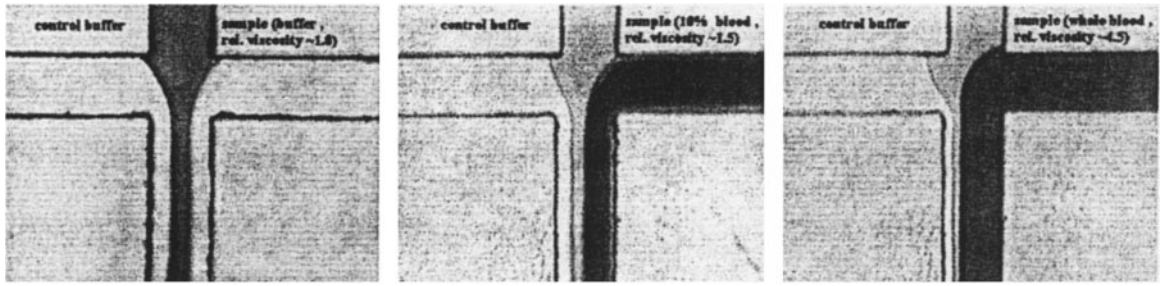

Fig. 8. Comparison of flow properties of buffer solutions (left), 1:10 diluted whole blood (middle), and undiluted whole blood (right). Experiment performed at 1 g, with the observation axis vertical

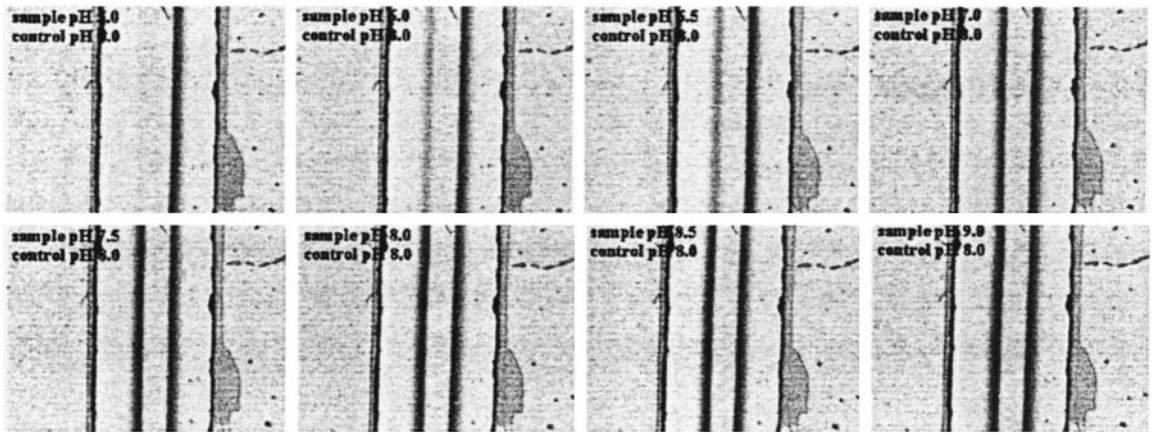

Fig. 9. Images of the same detection region in a T-Sensor for different pHs. Experiment performed at 1 g, with the observation axis vertical

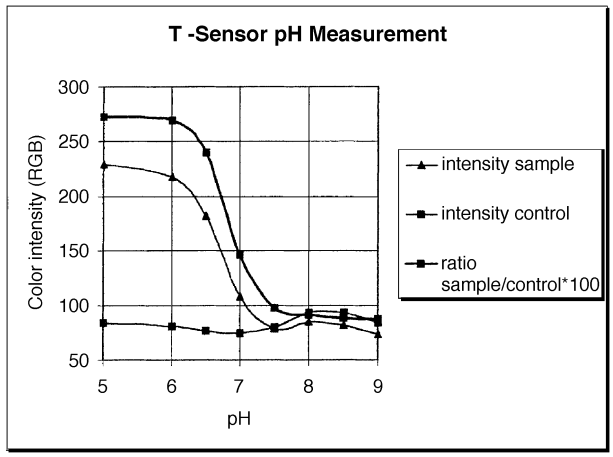

Fig. 10. Calibration curve generated from the image series in Fig. 9. Taking the ratio between sample and control interaction zone intensities compensates for most typical variations in experimental conditions (temperature, light source stability, flow rate, indicator photobleaching). The intensity is given as an averaged value of pixel intensity in each of the three RGB (red-green-blue) channels of the CCD camera

drive equal volumes of all three solutions through the structure. Since solutions with higher viscosities flow more slowly, they take up more of the cross-sectional area in the channel. This effect demonstrates that for known volume flow rates, the viscosity of a sample can be determined by measuring the locations of the interface lines, which depend on the changes in diffusion rates caused by variations in sample viscosity.

Figure 9 shows a series of images of the same detection region in a T-Sensor for different pH values. In each image, the control solution (a 0.1 M HEPES buffer at pH 8) enters the structure from the right, the indicator (a Bromocresol Purple solution) enters from the top, and the samples (0.1 M HEPES buffers ranging from pH 5 to pH 9) enter from the right. The images show that the color intensity of the sample interface line increases with pH, while the control interface line remains constant for all samples. The image series in Fig. 9 was used to generate the calibration curve shown in Fig. 10, by use of the image processing and data reduction procedures outlined in the experimental section. The curve ''intensity sample'' represents the integrated 8-bit RGB (averaged Red-Green-Blue pixel intensity in the CCD camera) value for the interaction zone between sample and indicator. The curve ''intensity control'' represents the control interaction zone. The ''ratio control/sample'' compensates for variations in light intensity, flow rate stability, temperature changes, and any other adverse conditions that affect both sample and control solution at the same time. It can be seen that the raw sample intensity values for pH 8 and 8.5 appear too high, but the ratio curve displays a typical sigmoidal pH calibration curve.

Microgravity Experiments

The goal of the microgravity T-Sensor experiments was twofold. First, we tried to validate the performance of this microfluidic diagnostic device under various accelerational forces. Such variations would have to be accommodated in space medicine, as well as in civil and military emergency medicine. Red blood cells are appreciably denser than the plasma and therefore settle at a rate of 1 μm/s at 1 g. Second, we

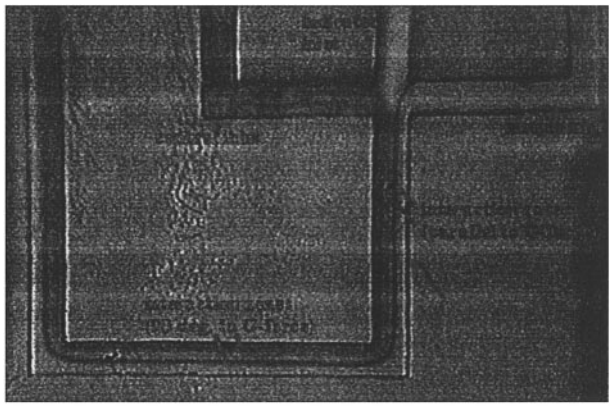

Fig. 11. T-Sensor in microgravity: sample (buffer with unknown pH), indicator (Bromocresol Purple), and control (buffer pH 6.5) from two interaction lines along the detection channel

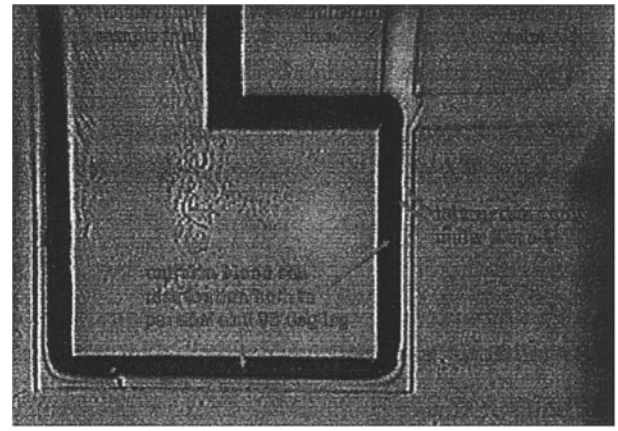

Fig. 12. Whole blood measurement in a T-Sensor in microgravity: an undiluted whole blood sample, indicator (Bromocresol Purple), and control (buffer pH 6.5) form two interaction lines along the detection channel. The whole blood layer takes up more area because of whole blood's higher viscosity

tried to determine whether the settling of blood cells in a T-Sensor under varying gravitational forces can be visualized, and to what extent it would cause a problem during measurements.

Figure 11 shows a T-Sensor operating under microgravity. The sample (a buffer with unknown pH), indicator (Bromocresol Purple), and control (0.1 M HEPES buffer, pH 6.5) form two interaction lines along the detection channel. The channel cross-section is $500\,\mu m \times 100\,\mu m$. The detection channel was U-shaped so that, under the influence of acceleration, the diffusion direction (perpendicular to flow) would first be perpendicular to, then parallel to, then finally perpendicular to gravity. The middle section represents the ''worst case'' for possible effects of acceleration on the device. Repeated measurements of interaction line intensity and location at both 1.8 g and at microgravity showed no significant variation due to the influence of gravity. The flow pattern in a T-Sensor with only buffers as samples, recorded at microgravity, was indistinguishable from that recorded at 1.8 g.

Figure 12 shows a repetition of these experiments, but with undiluted whole blood introduced into the sample inlet (left inlet in the figure). Because of the higher viscosity of whole blood, the flow lines were shifted to the left (see also Fig. 8). As expected, blood cells did not show any tendency to settle during the microgravity phase. A slight, but significant increase in blood cell density, however, was found at the lower left corner of the horizontal T-channel during the 1.8 g increased gravity phase of the flight parabolas. However, we found that at the pump speeds used for these experiments, blood cells did not sediment significantly across the channel. Therefore, the determination of the diffusion interaction zone intensities, and thus the determination of the blood pH, was not affected by changes in gravity between 0 and 1.8 g.

Conclusions

The T-Sensor and its variants presented in this paper allow the optical detection and assay of an analyte concentration in very small sample volumes and at correspondingly small sample stream flow rates. The sample stream may be composed of a ''clean'' carrier fluid or a turbid particle-laden fluid containing diffusing analytes. By coupling T-Sensors to an optical detector (e.g. a CCD or a set of multi-wavelength detectors) it should be possible to accurately determine the concentration of multiple analytes in body fluids such as blood, urine, and spinal fluid. Either absorbance or fluorescent indicator dyes may be used. Such devices have quantitative utility, can be easily mass-produced, and have many potential applications in clinical laboratory instruments.

In this paper, we have demonstrated quantitative determination of blood pH. Quantitative determination of several other analytes, including human serum albumin and calcium, as well as the feasibility of T-Sensor determination for a series of clinically significant analytes, including enzymes, electrolytes, blood

gases, proteins and drugs, such as total and ionized calcium (fluorescence and absorption), salicylate (absorption), and alkaline phosphatase (kinetic absorption) will be reported elsewhere.

It was also demonstrated that the T-Sensor can be used as a blood diagnostic tool regardless of the strength and orientation of gravity (0–1.8 g). Although blood cells sediment in a gravitational field, we found that at the pump speeds used for these experiments, blood cells did not move significantly across the channel, and did not impede a quantitative analysis T-Sensor-based instrumentation therefore has potential for space medicine and emergency medicine, as well as for more routine applications for which rugged and portable medical analyzers are required.

This work illustrates several features of using a T-Sensor and its self-referencing variant for chemical analysis, which have previously been advanced theoretically [13, 15] as follows.

(a) Analyte concentrations in turbid and strongly colored solutions, such as blood, can be determined optically without the need for preprocessing such as blood cell removal by centrifugation.

(b) Many standard optically-based (fluorescence or absorption) and electrochemical analytical methods may be performed within the T-Sensor.

(c) In many cases, indicator dye cross-sensitivity to larger sample particulates can be avoided in the T-Sensor by making use of the size-based diffusion separation feature of T-Sensors.

(d) For large analyte molecules (e.g. proteins), the diffusion of indicator molecules into the sample and reference streams may exceed the diffusion of analyte molecules into the detection stream. In this case, only the portions of the diffusion interaction zones facing towards the indicator stream are free from cross-sensitivity to sample and reference properties. By coupling the indicator molecules to large carrier molecules or beads, the diffusion of indicator molecules into the sample can be largely avoided.

(e) In a T-Sensor, the indicator dye and/or the detection chemistry can be kept in a solution formulated to display optimal characteristics of the detection reaction without affecting the chemical composition and equilibrium in the sample solution. For example, cross-sensitivities of pH or ionic strength can be suppressed by using strongly buffered solutions.

(f) The location of the diffusion boundaries yields information about flow speed, sample viscosity, sample concentration, dye diffusivity, analyte diffusivity, and dye dynamic range.

(g) The steady-state nature of this method makes long signal integration times possible. This can provide for higher sensitivities than those attainable with comparable flow detection systems.

(h) In a self-referencing T-Sensor, a control or reference solution containing a known or constant concentration of sample analyte can be analyzed in parallel within the same channel as the sample. This allows real-time referencing and control determination. Therefore, it is possible to compensate for effects such as variations in flow cell geometry, temperature dependent reaction kinetics, light source stability, instabilities in the optical system and detection electronics, as well as fluid parameters such as turbidity, color, concentration of detection chemistry, viscosity, and flow speed. As with all calibration and reference systems, the closer a reference solution resembles the sample solution, the better the referencing will be. Of particular importance for the T-Sensor are the viscosity and optical parameters of sample and reference. However, some variations between the two solutions can be compensated by using sophisticated T-Sensor imaging algorithms.

(i) Measuring the concentration of the analyte at several locations along the channel may provide a additional means to compensate for residual cross-sensitivities.

(j) Monitoring signal intensities along the T-Sensor detection channel (in the direction of flow) provides a means for looking at the kinetics of a reaction, thus allowing kinetic diagnostic reactions to be studied not as a function of time but of distance from the starting point of the diffusion interaction.

(k) It is possible to flow more than three separate streams through a single T-Sensor, allowing, for example, real-time analysis of a simple, as well as a low and high control.

(l) It is possible to determine two or more different sample analyte concentrations in one single T-Sensor, allowing, for example, the determination of ionized calcium in whole blood while simultaneously compensating for variations in the pH of the blood sample, which affects ionized calcium readings.

(m) T-Sensor manufacturing is not limited to silicon micromachining. Several other methods have been demonstrated that yield low-cost mass-manufacturable microstructures with similar sizes and geometries.

Acknowledgments. This work was supported by Micronics, Inc., Redmond, WA, DARPA (grant # DAMD17-94-J-4460), and the Washington Technology Center, Seattle, WA. We would like to thank CaiCai Wu, Margaret Kenny, and, in particular Diane Zebert, Mark Holl, and Wayne Breidford, for many helpful suggestions and practical help with the experimental setup. the microgravity experiments were performed with the support of NASA at their microgravity test facilities in Houston, TX under partial support of a grant of JK and KJM. We would like to thank Bob Williams and Burke Fort of NASA for their technical assistance. We would also like to thank Dr. James Brody, and the rest of the DARPA/former Portable Stat Lab Team at the University of Washington for active input and many helpful discussions. Two of the authors, Bernhard H. Weigl and Paul Yager, are required to note that they have ''significant financial interest'' in Micronics, Inc., Redmond, WA, USA.

References

[1] J. J. Cefai, D. A. Barrow, P. Woias, E. Muller, *J. Micromech. Microeng.* **1994**, *4*, 172.

[2] J. P. Brody, P. Yager, *Low Reynolds Number Micro-Fluidic Devices, Solid-State Sensor and Actuator Workshop*. Transducers Research Foundation, Hilton Head Island, South Carolina, 1996.

[3] A. Manz, C. S. Effenhauser, N. Burggraf, D. J. Harrison, K. Seiler, K. Fluri, *J. High Res. Chromatogr.* **1993**, *16*, 433.

[4] D. J. Harrison, *Science* **1993**, *261*, 895.

[5] A. Einstein, *Investigations on the Theory of the Brownian Movement* (R. Furth, Ed.) Dover Publishing, 1956, p. 122.

[6] M. Elwenspoek, T. S. J. Lammerink, R. Miyake, J. H. J. Fluitman, *J. Micromech. Microeng*. **1994**, *4*, 227.

[7] P. Gravesen, J. Branebjerg, O. S. Jensen, *J. Micromech. Microeng*. **1993**, *3*, 168.

[8] R. Zengerle, M. Richter, *J. Micromech. Microeng.* **1994**, *4*, 192.

[9] J. Happel, H. Brenner, *Low Reynolds Number Hydrodynamics*, 2nd Ed. Noordhoff, Leyden, 1973, p. 553.

[10] E. L. Cussler, *Diffusion, Mass Transfer in Fluid Systems*. Cambridge University Press, Cambridge, 1984, p. 525.

[11] M. A. Afromowitz, J. E. Samaras, *Sep. Sci. Tech.* **1989**, *24*, 325.

[12] B. H. Weigl, P. Yager, *Sens. Actuators B* **1997**, *39*, 452.

[13] B. H. Weigl, M. Holl, D. Schutte, J. P. Brody, P. Yager, *Anal. Meth. Instrum.* **1996**, μTAS '96 special Issue.

[14] P. Yager, B. H. Weigl, M. Holl, J. P. Brody, *Microfabricated Diffusion-Based Chemical Sensor*, US Patent No 5716852, issued 1998.

[15] P. Galambos, F. K. Forster, B. H. Weigl, *Transducers 97* (International Conference of Solid-State, Sensors and Actuators), Digest of Technical Papers **1997**, *1*, 535.

Received May 22, 1998. Revision November 10, 1998.